Analysis of the Structure and Mass Transport Properties of Clay Nanocomposites Based on Amorphous PET

A. Greco, C. Esposito Corcione, A. Strafella, A. Maffezzoli

Department of Engineering for Innovation, University of Salento, Lecce, Italy

Received 3 November 2009; accepted 6 March 2010
DOI 10.1002/app.32401
Published online 15 July 2010 in Wiley InterScience (www.interscience.wiley.com).

ABSTRACT: The aim of this work is to characterize the rheological and permeability behavior of nanocomposites based on amorphous poly(ethylene terephthalate) (PETg) and organically modified montmorillonites (omMMT), obtained by melt intercalation. The use of PETg instead of semicrystalline PET is believed to reduce the risks associated to organic modifier degradation during processing at high temperatures. X-ray and transmission electron microscopy analysis performed on the PETg nanocomposites showed that processing for long time at temperatures lower than melting of semicrystalline PET allowed to obtain a partially intercalated structure with some degree of exfoliation. The rheological behavior of PETg nanocomposites was studied as a function of shear rate in a cone–plate rheometer in order to correlate the viscosity with the aggregation state of omMMT. A simple model accounting for an apparent increase of rheological units size, associated with the intercalation of PETg macromolecules into omMMT galleries, is proposed. The glass transition temperature, T_g, as a function of the volume fraction of omMMT content of the nanocomposite, was measured using differential scanning calorimetry. Finally, the water vapour permeability of PETg nanocomposites was correlated to the volume fraction of the impermeable inorganic part of the omMMT. © 2010 Wiley Periodicals, Inc. J Appl Polym Sci 118: 3666–3672, 2010

Key words: PETg; omMMT; nanocomposites; permeability

INTRODUCTION

Poly(ethylene terephthalate) (PET) is a low-cost commodity polymer that finds use in a wide variety of applications, such as fibers, bottles, films, and even engineering plastics for automobiles and electronics. Incorporation of nanodispersed clay in PET can have a significant impact on PET properties, improving flame resistance, oxygen barrier properties, and elastic modulus.[1–3] To enhance the "compatibility" between the nanofiller and the polymer, thereby improving the extent of exfoliation and the related nanofiller dispersion within the polymer, it is often necessary to modify the chemical structure of the surface layers of natural occurring silicate fillers. For the case of thermoplastic matrix nanocomposites the intercalation of the nanofiller is usually carried out by conventional melt-compounding methods. Melt intercalation of the layered silicate by PET requires high temperatures, which can induce considerable degradation of the organic modifier through chemical decomposition reactions, which may result in extensive deterioration of the interfacial interactions between the filler and the polymer.[3–6] PET/clay nanocomposites prepared through melt intercalation method have resulted in very limited intercalation of guest molecules.[7] As a consequence of this, PET nanocomposites can be efficiently obtained using highly thermally stable surface modified organoclay,[6] which in turn increases the cost of the nanofiller. Alternatively, PET nanocomposites can be prepared by *in situ* interlayer polymerization of monomers[8–10] or of cyclic oligomers.[7] The polymerization must be run in controlled conditions, requiring very extensive purging of the material and high vacuum, and very often final washing to remove impurities of by-products of the reaction.[7,8] Further, the ineffective control of the stoichiometry leads to the formation of low molecular weight PET.[7] Finally, the times required for producing nanocomposites by *in situ* polymerization are much higher than the typical times required to produce nanocomposites by melt intercalation.

On the other hand, amorphous PET (PETg), obtained by adding cyclohexane dimethanol in place of ethylene glycol[11] is a clear amorphous polymer, which is extensively used in flexible packaging[12] and in composite industry for the production of hybrid yarns (Comfil®). Compared to semicrystalline PET, the PETg offers a broader range of processing parameters,[13] which, in composite industry, allows for cycle reduction. PETg matrix nanocomposites were efficiently prepared by melt intercalation[11,12] and studied mainly concerning their relaxation behavior by calorimetric and dielectric

Correspondence to: C. E. Corcione (carola.corcione@unile.it).

characterization. On the other hand, no report of the rheological properties of the nanocomposite, which are very important in determining the processability of nanocomposite, can be found in literature. Since PETg and semicrystalline PET are miscible, the development of a nanodispersed PETg matrix masterbatch could find application as an intermediate step to promote nanodispersion of organically modified Montmorillonite (omMMT) in PET. The PETg nanocomposite would be mixed for a very short time with PET dramatically reducing the risk of degradation of the organic modifier of omMMT and at the same time introducing a low-cost nanofiller in the amorphous phase of PET with an expected improvement of PET barrier properties. To find applications as high-barrier properties materials, the permeability of PETg nanocomposites needs also to be studied and analyzed. To the best of our knowledge, no work dealing with the barrier properties of PETg nanocomposite is reported in literature.

In this work, PETg nanocomposites at high nanofiller content (10 and 20% by weight) were produced by melt mixing of amorphous PETg with organically modified montmorillonite clay at 150°C for 1 h. Nanocomposites were characterized by X-ray diffraction, rheological, thermal, and mechanical analysis. In particular, the viscosity of the PETg/omMMT nanocomposites was correlated with the aggregation state of omMMT. A simple model accounting for an apparent increase of rheological units size associated with the intercalation of PETg macromolecules into omMMT galleries, is also proposed. The permeability of the PETg/caly nanocomposite to water vapour was then measured.

EXPERIMENTAL

The material used as matrix was an amorphous PET (PETg), shrink film from Eastman Embrace, with an intrinsic viscosity of 0.70 dl/g, and density of 1.30 g/cm^3. The nanofiller was a Montmorillonite (MMT) modified with 28% w/w dimethyl benzohydrogenated tallow; tradename Dellite 43 B (omMMT), supplied by Laviosa, Italy. All materials were dried for 8 h at 80°C before compounding.

The PETg nanocomposites were prepared by melt mixing PETg with omMMT in a batch mixer (Thermo-Haake) Rheomix 600 at 150°C for 1 h, under a nitrogen flux of 60 μL/min. The nanofiller content was set at 10 and 20% by weight, as reported in Table I.

X-ray analysis was performed on both nanofiller and nanocomposite powders, within the range $2\theta = 1^\circ - 10^\circ$, using a Wide angle X-ray Diffractometer, RIGAKU Ultima +.

TEM measurements were performed on nanocomposites using a high-resolution transmission electron microscope (TECNAI G^2 F30), with an accelerating voltage of 300 kV. Nanocomposite ultrathin sections of about 90 nm were cut by a microtome equipped with a diamond knife and placed on a copper grid.

TABLE I
Weight and Volumetric Composition of PETg/omMMT Nanocomposites

Sample	Weight fraction (%)	Volume fraction (%)
Nano10	90 PETg/ 10 omMMT	89.79 PETg/ 10.21 omMMT
Nano20	80 PETg/ 20 omMMT	79.62 PETg/ 21.38 omMMT

Differential scanning calorimetry (DSC) was performed on a Perkin Elmer DSC 7 instrument under a nitrogen flux at 30 mL/min. The materials were heated at 10°C/min from room temperature to 270°C and then cooled down to room temperature. Afterwards, the sample were subjected to a second heating scan at 10°C/min to 270°C.

Rheological analysis was performed on an ARES instrument. Materials were tested with a cone and plate geometry between 0.1 and 10 s^{-1} at 270°C.

Permeability tests were performed by the dish method according to the ASTM E 96 using anhydrous calcium chloride as desiccant. Circular samples characterized by a thickness of 0.32 + 0.02 mm and a diameter of 60 mm were obtained by compression molding, and dried at 65°C under vacuum for 48 h. The permeability to water vapor was measured at 50°C and 60% relative humidity. The transmission rate was normalized with respect to the film thickness. Water vapor permeability P [g mm/Pa m^2 s] was obtained from eq. (1) according to the ASTM E 96:

$$P = \frac{\dfrac{G}{t \cdot A}}{\dfrac{S \cdot (R_1 - R_2)}{100}} \cdot \delta, \qquad (1)$$

Where δ is the thickness of the film, G is the weight gain of the polymer film, t is the time during which G occurred, A is the test area, S is the saturation vapor pressure at test temperature (123.5 mmHg), R_1 is the relative humidity in the test chamber, R_2 is the relative humidity at the dry side of the film, which was taken equal to zero.

RESULTS AND DISCUSSION

The X-ray diffraction traces of the PETg/omMMT nanocomposites are reported in Figure 1. The omMMT shows a main diffraction angle at 4.7°, corresponding to about 1.85 nm lamellar spacing. After mixing with the PETg, the diffraction peak is shifted to about 2.5°, which indicates an increase of the lamellar spacing and, therefore, the presence of an intercalated structure. No significant difference can

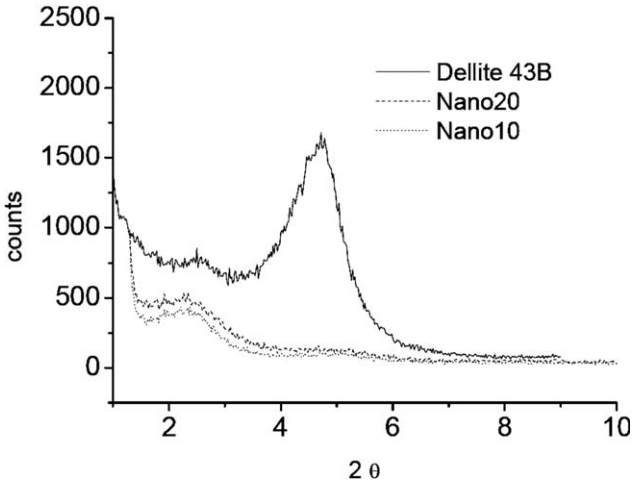

Figure 1 X-ray traces of omMMT and nanocomposites with PETg.

be observed for the samples with two different omMMT content. The small shoulder present at 4.7° for samples Nano10 and Nano20 indicates that a small fraction of omMMT was still not intercalated. A longer processing time could be probably required to achieve optimum exfoliation of the nanofiller.

The TEM micrograph of sample Nano20, reported in Figure 2, shows the presence of a regular stacking arrangement of the clay layers. Lamellar stacks of omMMT are well dispersed in the polymer matrix, being omMMT layers still organized in a parallel way, although their basal spacing is much higher in the composite in comparison to the neat sample, as the layers are irregularly separated by about 3.4 nm of polymer. This finding is in very good agreement with X-ray analysis results, evidencing the formation of an intercalated nanocomposite. The presence of some single clay layers homogenously dispersed in the polymer matrix, evidenced in Figure 2, indicates the formation of a partially exfoliated nanocomposite.

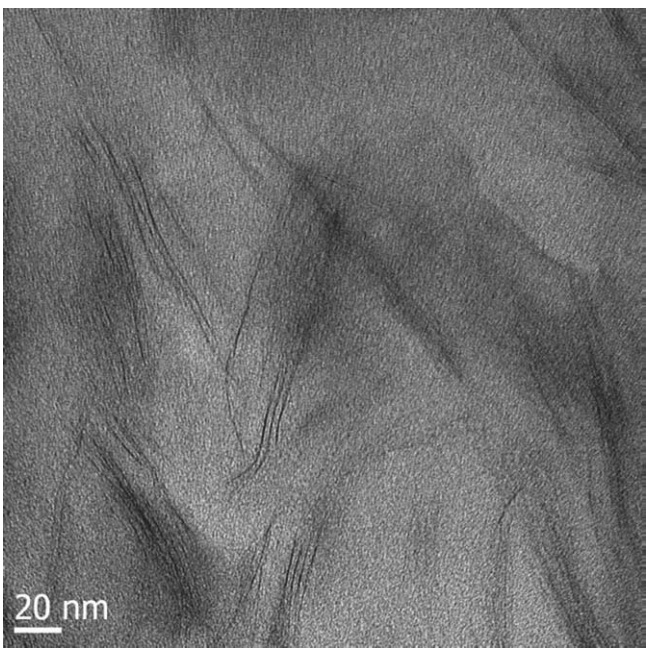

Figure 2 TEM analysis for sample Nano20.

The good intercalation of the nanofiller was also confirmed by rheological analysis results, reported in Figure 3. As it can be observed, at shear rate = 0.1 s^{-1}, the viscosity of the PETg increases by a factor of 40 after the addition of 10 wt % of nanofiller (Nano10). Further addition of the 10% nanofiller (Nano20) causes another increase to about 50 times the initial viscosity of PETg, at the same shear rate.

A simple expression which well describe the fluid behavior in steady shear rheological experiments, is the empirical "power law equation"[14]:

$$\eta = K\dot{\gamma}^{(n-1)}, \qquad (2)$$

Where η is the fluid viscosity at shear rate $\dot{\gamma}$, and K and n are model parameters, generally referred to as consistency and flow index, respectively. Equation (2) can be applied for $\dot{\gamma}$ values comprised between upper and lower Newtonian plateau regions.

The shear rate dependence of PETg/ omMMT viscosity was modeled using eq. (2). Results for the fitting parameters are reported in Table II. The value of K determined for each sample, normalized to the value of K determined for PETg is also reported in Table II. As it can be observed, the consistency index K/K_{PETg} increases with increasing nanofiller content. Also, the flow index of the nanocomposites is much lower than that of the neat matrix, indicating a strongly non-Newtonian behavior of the PETg nanocomposites.

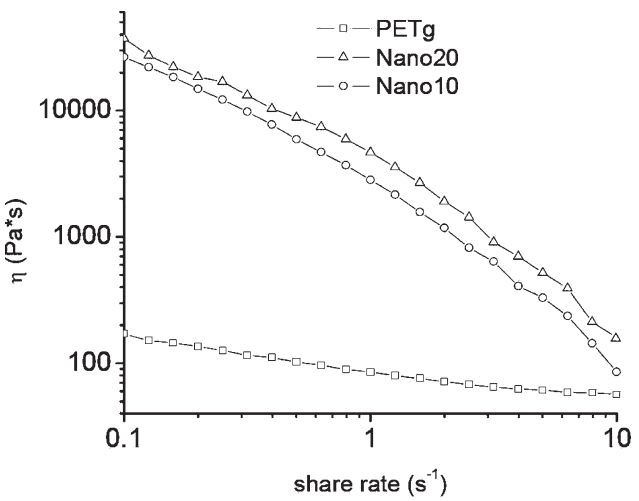

Figure 3 Stationary viscosity curves for PETg and samples Nano10 and Nano20.

TABLE II
Fitting Parameters of "Power Law Equation"

Weight fraction (%)	K/K_{PETg}	n
PETg	1 ± 0.011	0.73 ± 0.0076
Nano 10	35.96 ± 1.30	0.065 ± 0.0018
Nano20	50.18 ± 1.24	0.094 ± 0.002

The dependence of the viscosity of PETg/omMMT systems on the volume fraction of omMMT was also modeled. The rheology of multiphase systems, and more specifically of solid–liquid suspensions, was the object of many investigations, both theoretical and experimental, starting from the work of Einstein.[14–16]

The Einstein equation can be applied to very dilute suspensions (solid volume fraction $\Phi < 0.02$) of rigid spheres in a Newtonian fluid[14,16]:

$$\eta_r = 1 + 2.5 * \Phi, \tag{3}$$

Where η_r is the relative viscosity of the suspension, calculated as the ratio between the viscosity of the filled suspensions, η, and the viscosity of the suspending medium, η_s.

The classical equation of Einstein was generalized in order to include: (a) the effect of viscoelasticity of the particles[5]; (b) the nonzero Reynolds number corrections[6]; (c) the deformability of the particles[7]; (d) the nonspherical shape of particles[8]; (e) the sedimentation process of the filler.[9] Starting from Einstein equation, a large number of correlations between the relative viscosity, η_r, and the volume fraction of the solid particles, Φ, were published in the literature.[10] These theoretical models derive from three assumptions: (1) the diameter of rigid particles is large compared to the suspending medium molecules, but small compared to the smallest dimension that can be measured by the rheometer; (2) flow is at steady state without inertial concentration gradient or wall slip effects; and (3) the medium liquid adheres perfectly to particles.[14] There may be also a fourth assumption taking into account the interparticle interaction, depending on the model chosen.

Among these equations, we found that a good fit of our experimental data by using Batchelor expression:

$$\eta_r = 1 + k_1 * \Phi + k_2 * \Phi^2. \tag{4}$$

Equation (4) is obtained from the classical Einstein model, eq. (3), operating a correction that takes into account the effect of more concentrated suspensions of particles (solid volume fraction $\Phi > 0.02$).[7] In particular, referring to the physical significance of the parameters introduced in eq. (4), k_1 accounts for the shape of the particles in suspension. According to Einstein equation, k_1 equals to 2.5 for spherical particles, whereas in the case of nonspherical particles Guth found that k_1 depends on the aspect ratio p, according to[8]:

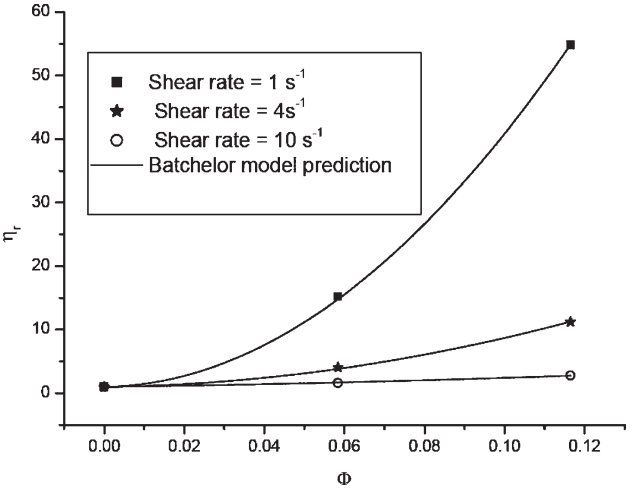

Figure 4 Comparison between experimental data and Batchelor model prediction.

$$k_1 = \frac{p}{2\ln(2p) - 3} + 2. \tag{5}$$

According to Fornes and Paul[17] the aspect ratio of a single layer of omMMT as measured by transmission electron microscopy is about 120. By substituting this values in Eq. (5), a value of k_1 can be calculated. For the results reported in Figure 2, at each value of shear rate the nanofiller content dependence of viscosity was fitted with Batchelor equation. As an example, a comparison between experimental data and Batchelor model prediction, in correspondence of shear rate values of 1, 4, 10 s^{-1}, is reported in Figure 4. The values of the parameter k_2, obtained by nonlinear fitting are reported in Table III as function of the shear rate. The calculated values of k_2 are very high in comparison with those reported in the literature,[14,10] which is probably due to the nanometric nature of the filler used. In fact, the values of k_2

TABLE III
The Values of the Parameter k_2 of Batchelor Model Prediction

$\dot{\gamma}$ (s^{-1})	k_2 [KPa s]
0.1	15980.24 ± 173.21
0.5	6293.97 ± 58.69
1	3900.37 ± 22.48
3	892.69 ± 14.59
4	634.76 ± 11.47
5	480.01 ± 11.65
6	342.09 ± 2.57
8	121.84 ± 3.37
10	57.64 ± 4.37

TABLE IV
Fictive Molecular Weight of Nanocomposites as Function of omMMT Volume Fraction

Φ	M_{wf} (g/mol)
0	8.7×10^4
0.058	4.8×10^6
0.12	1.9×10^7

usually reported in literature are relative to micrometric filler, for which the polymer-filler interactions are much lower than those characteristic of nanofillers. The decrease of k_2 with the shear rate can instead be attributed to some orientation of the nanofiller lamellae during the flux, which involve a decrease of the physical interactions between omMMT lamellae.

The increase of viscosity induced by the nanofiller can be attributed to the formation of large rheological units of PETg chain segments coordinated by several omMMT lamellae. omMMT is therefore responsible of the aggregation of PETg chains which behaves as larger and entangled polymer molecules with a fictive higher average molecular weight, with respect to the unfilled PETg. Therefore a fictive equivalent molecular weight M_{wf} can be associated to the presence of omMMT lamellae in the PETg. The viscosity of nanofilled PETg can be related to the fictive molecular weight by using an expression similar to the Mark-Houwink equation[14]:

$$\eta_0 = kM_{wf}{}^a, \tag{6}$$

Where k is a model parameter depending on the nature of the polymer and on the temperature and finally a is a model parameter, assumed equal to 3.4 for many polymers.[14] Usually, η_0 is taken as the zero shear rate viscosity. In this work, we have used the shear rate evaluated at 0.1 s^{-1}. By substituting the Batchelor equation into the expression derived by the Mark-Houwink equation, the following relation between fictive molecular weight and nanofiller content can be obtained:

$$M_{wf} = k_3 * (1 + k_1 * \Phi + k_2 * \Phi^2)^{1/a}, \tag{7}$$

Where k_3 is the average molecular weight of unfilled PETg. The latter was estimated from measured intrinsic viscosity using Mark-Houwink parameters by Hu et al. and it is equal to 87,000 g/mol.[18] The value of a was taken equal to 3.4.[14] Finally, experimental viscosity data measured at 0.1 s^{-1} were used to calculate the fictive molecular weight of nanocomposites, taking $k_1 = 8.5$ and $k_2 = 15980$. The results reported in Table IV show that the incorporation of the nanofiller involves the formation of very large rheological units corresponding to a huge increase of the fictive molecular weight.

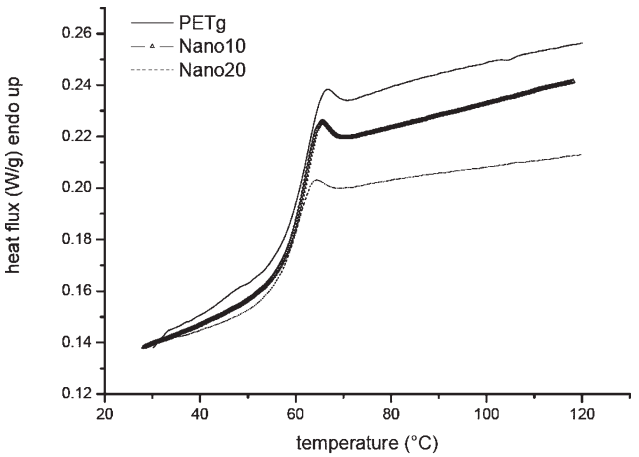

Figure 5 DSC curves for PETg and samples Nano10 and Nano20.

The glass transition temperature T_g of PETg/omMMT nanocomposites was measured using differential scanning calorimeter (DSC). The results for PETg filled with different amount of omMMT are reported in Figure 5. The curves are obtained during a second heating after cooling down from 300 to 25°C at 10°C/min.

The PETg is completely amorphous, with a T_g of about 68.1°C. After addition of the nanofiller, T_g decreases to 67.1°C and to 66.00°C, respectively for the sample with 10 wt % and 20 wt % of Dellite 43B. The absence of any other exothermal or endothermal signal confirms that also the nanocomposite is amorphous. This is in agreement with the results reported by Kattan et al.[13], who observed that the PETg keeps its amorphous state in most practical experimental conditions. Different factors can affect the T_g

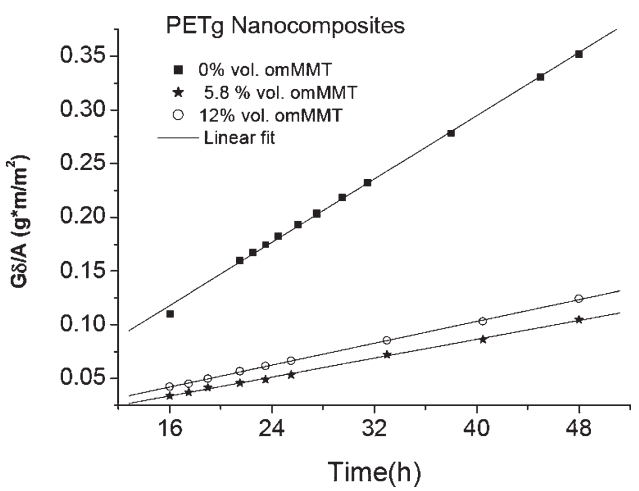

Figure 6 Amount of water permeated through the PETg and PETg nanocomposites normalized to the sample geometry [G δ/A of eq. (1)].

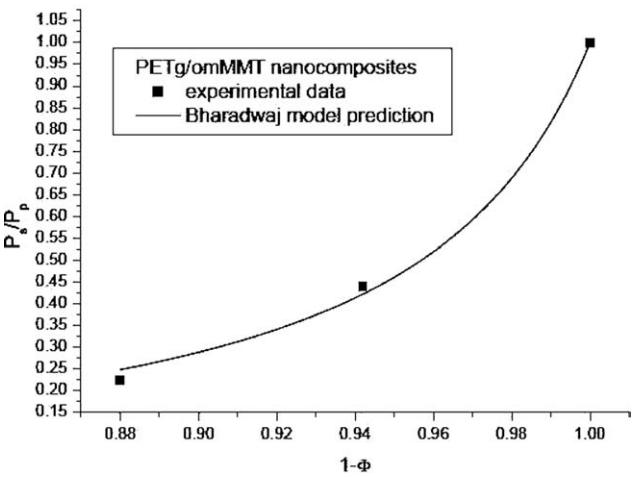

Figure 7 Water vapor permeability of PETg/omMMT nanocomposites (P_s) normalized to permeability of unfilled PETg (P_p) versus omMMT volume fraction (Φ).

decrease. Among these, the processing conditions and the presence of the organic modifier of the MMT are characterized by a very low T_g.

Finally, permeability measurement were performed according to the method described above. The amount of water permeated through the PETg and PETg nanocomposites normalized to the sample geometry [$G\ \delta/A$ of eq. (1)] is reported in Figure 5.

After a nonsteady state time interval measured before 16 h for all samples, a linear weight increase is observed, indicating that the steady state conditions are achieved. The raw data of Figure 5 were then used to calculate the water vapour permeability according to eq. (1). The water vapor permeability of PETg/omMMT nanocomposites (P_s) normalized to permeability of unfilled PETg (P_p) is reported in Figure 6 as a function of the omMMT volume fraction (Φ). The permeability decreases with increasing nanofiller content, due to the presence of inorganic impervious filler, and to a longer diffusive path of the penetrant dependent on filler size and orientation. The nonlinear dependence of P on Φ can be fitted using Bharadwaj equation[19]:

$$\frac{P_s}{P_p} = \frac{1-\Phi}{1+\frac{L}{2W}\Phi\left(\frac{2}{3}\right)\left(S+\frac{1}{2}\right)}. \quad (8)$$

Where:

P_s = permeability of the PETg/omMMT nanocomposites

P_p = permeability of the pure PETg

L/W = aspect ratio, assumed equal to 120[14]

$S = \frac{1}{2}(3\cos^2\vartheta - 1)$= orientational order

with θ = angle between the direction of preferred orientation (n) and the sheet normal unit vectors p.

The results are reported in Figure 7.

The orientational order S can range from 1 (θ = 0°), indicating perfect orientation of the sheet normal unit vectors p with n, to −0.5 (θ = 90°), indicating perpendicular or orthogonal orientation, and a value of 0, indicating random orientation of the sheets.

In this case $S = 0.03$ (corresponding to θ = 53.5°) indicates an almost random orientation of omMMT lamellae induced by compression molding, where negligible shearing occurs, of film samples used for permeability measurements. Different permeability results, either higher or lower, could be obtained in dependence of the orientation of omMMT lamellae with respect to the direction of diffusion.

CONCLUSIONS

In this work PETg matrix/omMMT nanocomposites were obtained by melt compounding. A good intercalation of the nanofiller, with some degree of exfoliation, resulted from X-ray and TEM analysis, even when large amounts of omMMT were used. The incorporation of the nanofiller significantly increased the viscosity of the material, which is in turn attributed to an increase of the fictive molecular weight, associated to the formation of very large rheological units. The introduction of an impervious inorganic phase that increases the tortuosity of the path of a low molecular weight penetrant permeating through the nanocomposite, is responsible of a water vapour permeability reduction.

This amorphous PETg nanocomposites containing a large amount of nanofiller can be used as masterbatch for the development of semicrystalline PET/omMMT nanocomposites. This approach can overcome most of the difficulties encountered in PET nanocomposite production by melt intercalation:

- Surface modifier degradation: The use of an amorphous matrix for masterbatch production requires lower processing temperatures (as low as 150°C), which are more compatible with the thermal stability of nanofiller surface modifier.
- Intercalation of the nanofiller: The low mixing temperatures allow intensive mixing for sufficiently long times. Consequently, efficient intercalation of the nanofiller can be achieved.

References

1. Pegoretti, A.; Kolarik, J.; Peroni, C.; Migliaresi, C. Polymer 2004, 45, 2751.
2. Ray, S. S.; Okamoto, M. Prog Polym Sci 2003, 28, 1539.
3. Acierno, D.; Amendola, E.; Callegaro, G.; Napolitano, G. Macromol Symp 2007, 247, 120.

4. Acierno, D.; Scarfato, P.; Amendola, E.; Nocerino, G.; Costa, G. Polym Eng Sci 2004, 44, 1012.
5. Xiao, J.; Hu, Y.; Wang, Z.; Tang, Y.; Chen, Z.; Fan, W. Eur Polym J 2005, 41, 1030.
6. Davis, C. H.; Mathias, L. J.; Gilman, J. W.; Schiraldi, D. A.; Shields, J. R.; Trulove, P.; Sutto, T. E.; Delong, H. C. J Polym Sci Part B Polym Phys 2002, 40, 2661.
7. Lee, S. S.; Ma, Y. T.; Rhee, H. W.; Kim, J. Polymer 2005, 46, 2201.
8. Chang, J. H.; Kim, S. J.; Joo, Y. L.; Im, S. Polymer 2004, 45, 919.
9. Ke, Y.; Long, C.; Qi, Z. J Appl Polym Sci 1999, 71, 1139.
10. Wang, D. Y.; Wang, Y. Z.; Wang, J. S.; Chen, D. Q.; Zhou, Q.; Yang, B.; Li, W. Y. Polym Degrad Stab 2005, 87, 171.
11. Couderc, H.; Saiter, A.; Grenet, J.; Saiter, J. M.; Boiteux, G.; Nikaj, E.; Stevenson, I.; D'Souza, N. A. Polym Eng Sci, to appear.
12. D'Souza, N. A.; Ranade, A.; Gnade, B.; Ratto, J.; Thellen, C. In Flexible Packaging Conference; Amorphous PETG nanocomposites with montmorillonite, Barcelona, 2004; p 141.
13. Kattan, M.; Dargent, E.; Ledru, J.; Grenet, J. J Appl Polym Sci 2001, 81, 3405.
14. Utracki, L. A. Polymer Alloys and Blends, Thermodynamics and Rheology; Hanser Plublishers: New York, 1989.
15. Nicolais, L.; Astarita, G. Ing Chim Ital 1973, 9, 123.
16. Dealy, J. M.; Wissbrun, K. F.; Reinhold, V. Melt Rheology and Its Role in Plastics Processing: Theory and Applications; Van Nostrand Reinhold: New York, 1990.
17. Fornes, T. D.; Paul, D. R. Polymer 2003, 44, 4993.
18. Hu, Y. S.; Liu, R. Y. F.; Schiraldi, D. A.; Hiltner, A.; Baer, E. Macromolecules 2004, 37, 2136.
19. Bharadwaj, R. K. Macromolecules 2001, 34, 9189.